SQUID-based Thermometers

Jörn Beyer, Alexander Kirste and Thomas Schurig

Physikalisch-Technische Bundesanstalt (PTB)
Abbestr. 2-12, D-10587 Berlin, Germany

thomas.schurig@ptb.de

***Abstract* -This article reviews the application of SQUIDs in low-temperature thermometry. Special focus is given to state-of-the-art noise thermometers such as the current sensing noise thermometer (CSNT) and the magnetic field fluctuation thermometer (MFFT). Today, SQUID noise thermometers are no longer a domain of metrology institutes. Practical versions of the CSNT and the MFFT are powerful tools for relative primary thermometry in the low-temperature range down to sub-millikelvin temperature.**

***Keywords (Index Terms)* – low-temperature thermometry, SQUID, noise thermometer,**

Received: June, 20, 2016; Accepted: July 28, Day, 2016. Reference No. CR72; Category 4.

I. INTRODUCTION

SQUIDs can be used to design sensitive thermometers for temperature measurements in the low and ultralow temperature range. For this purpose, the SQUID is utilized to measure a physical quantity G, which is a function of the thermodynamic temperature T and a number of parameters x_i

$$G = f\left(T, x_1, x_2, \ldots\right) \tag{1}$$

The parameters x_i have to be determined, for example, by a calibration procedure, to calculate the temperature T from the measurand G.

Thermometers equipped with SQUIDs can be set up by using already well-established temperature measurement techniques or thermometers [1], for example, thermocouples, where the SQUID is simply used as a sensitive signal amplifier [2]. This can improve the sensitivity of a thermometric method significantly. On the other hand, the SQUID can be used to generate the quantity G itself or it can be an integral part of the thermometer setup which is

the case in resistive SQUIDs (RSQUIDs) and SQUID-based noise thermometers, respectively.

This article gives an overview of SQUID-based temperature measurement techniques with a focus on noise thermometry because the latter is currently the most important application of SQUIDs in practical low-temperature thermometry. In particular, the commercial availability of cryogen-free refrigerators for the temperature range $10\ \mathrm{mK} < T < 1\ \mathrm{K}$ has stimulated the development of robust and easy-to-handle SQUID noise thermometers for this temperature range. Meanwhile, even the first refrigerators based on adiabatic nuclear demagnetization cooling with dry precooling for sub-millikelvin temperatures have hit the market and, hence, appropriate practical thermometers for these coolers are required as well [3]. SQUID thermometers are promising candidates.

II. SOME BASIC METROLOGY ASPECTS

The basis for reliable practical thermometry is a well established and internationally agreed temperature scale. In the low-temperature range in which the refrigerators mentioned above operate, we are facing a situation where two independent temperature scales, the International Temperature Scale-1990 (ITS-90) and the Provisional Low Temperature Scale (PLTS)-2000, exist. The ITS-90 [4] ranges down to 0.65 K and is based on a ^{3}He vapor pressure scale in the temperature range 0.65–3.2 K. Since 2000, the PLTS-2000 for the temperature range from 0.9 mK to 1 K is in use [5]. This scale is based on the temperature dependence of the ^{3}He melting pressure and overlaps with the ITS-90 in the range 0.65–1 K, where the ITS-90 has been found to deviate systematically from thermodynamic temperature. Therefore, the Consultative Committee for Thermometry (CCT) of the International Bureau of Weights and Measures (Bureau International des Poids et Mesures, BIPM) recommends the use of the PLTS-2000 in the overlapping range of both scales [6]. Recently, the German National Metrology Institute (Physikalisch-Technische Bundesanstalt, PTB) has established a new ^{3}He vapor-pressure-based temperature scale from 0.65 K to 3.2 K, the PTB-2006 which removes the thermodynamic inconsistency of the ITS-90 below 1.2 K and which is consistent with the PLTS-2000 [7].

The national metrology institutes are currently working on a redefinition of the temperature unit kelvin based on a redetermination of the Boltzmann constant. So, in the near future, the temperature unit will be no longer dependent on a material property, the triple point of water, but on an unchangeable fundamental constant [8]. This redefinition will not affect the use of the existing temperature scales, and a change of the ITS-90 or the PLTS-2000 in the near future is not intended.

Nevertheless, for reliable temperature measurements in the low and ultralow temperature range, robust and easy-to-handle thermometers traceable to the PLTS-2000 with

an adequate uncertainty are required. As it will be shown below, novel SQUID-based noise thermometers are attractive devices fulfilling these requirements.

For metrology, in particular for establishing a temperature scale, so-called primary thermometers are very important instruments. An absolute primary thermometer [9] is characterized by a known single-valued function f of Eq. (1), where all the temperature independent parameters x_i can be obtained, either by definition or from independent measurements, and the thermodynamic temperature is directly related to the defined numerical value of the Boltzmann constant. Furthermore, this device must have a high metrological quality with respect to the uncertainty of the measurement and its reproducibility. A thermometer with a physically founded functional dependence of Eq. (1) but with at least one unknown parameter x_i, to be determined by calibration at one known temperature, is referred to as the relative primary thermometer [9]. Secondary thermometers, whose relation of the measurand and thermodynamic temperature is only inaccurately known, for example, resistance thermometers can be beneficially used for practical thermometry after a point-by-point calibration.

III. THE RESISTIVE SQUID NOISE THERMOMETER

The measurement of thermal noise is an attractive method for the determination of the thermodynamic temperature in a wide temperature range. In particular, the voltage noise of a resistor can be used for noise thermometry based on the well-known Nyquist formula

$$V_{\mathrm{N}}^2 = 4k_{\mathrm{B}}TR\Delta f \tag{2}$$

where V_{N}^2 is the mean square noise voltage across the terminals of a resistor with the resistance R at a temperature T. Δf is the bandwidth of the voltage measurement and k_{B} is the Boltzmann constant. If the relation $hf \ll k_{\mathrm{B}}T$ (h Planck constant) holds, quantum corrections can be neglected [1]. This is the case even for very low temperature in a wide frequency range, for example, $hf/k_{\mathrm{B}}T < 5 \times 10^{-4}$ for $T > 1$ mK and $f < 10$ kHz.

Noise thermometry was hampered for a long time by the fact that noise signals to be measured are very weak, notably at low temperature. When SQUIDs became available, the situation changed, at least for applications in metrology laboratories.

Kamper and Zimmermann [10] have introduced a special SQUID where the voltage noise-generating resistor is an integral part of the SQUID loop. This device, composed of the resistor, the superconducting parts of the loop, and a Josephson junction, is referred to as resistive SQUID or briefly RSQUID (Figure 1).

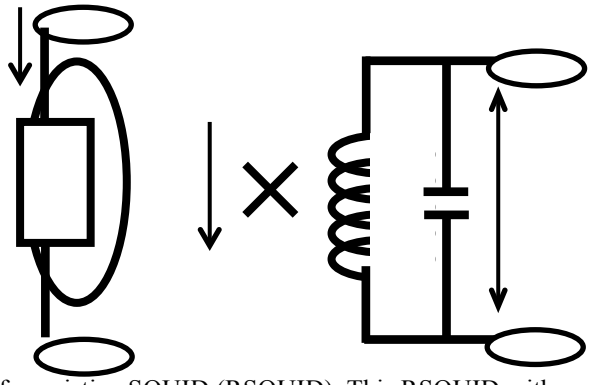

Fig. 1. Equivalent circuit of a resistive SQUID (RSQUID). This RSQUID with one Josephson junction is an rf RSQUID.

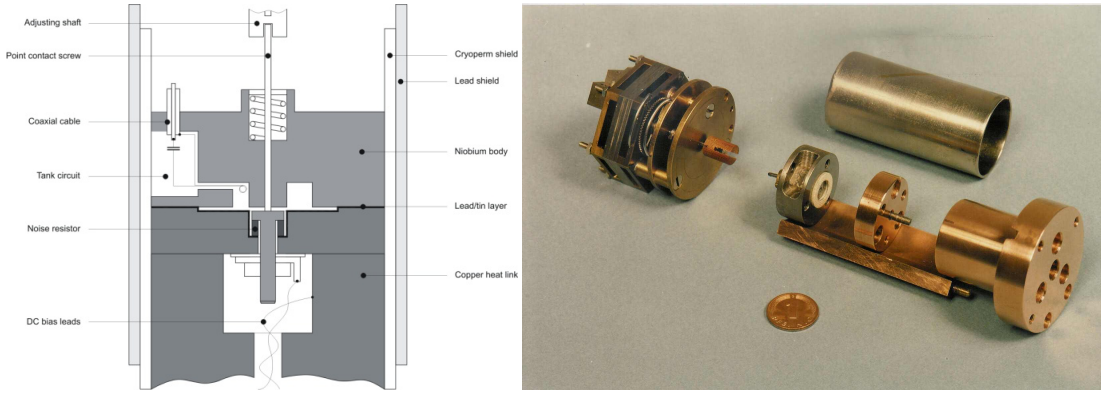

Fig. 2. rf RSQUID with mechanical point contact **[11]**. An adjustable niobium screw is pressed against a niobium body. For the noise resistor, a PdPtAu alloy with low absolute thermoelectric power and temperature coefficient of resistance is used. The superconducting loop is closed by a lead/tin solder layer covering the surface of an OFHC copper cylinder.

These devices have been developed and used in the 1970s and 1980s. They were built from bulk material and equipped with adjustable mechanical point contacts, as it is shown in Figure 2.

The RSQUID is working as a voltage-to-frequency converter. It transforms the voltage V_J across the resistor which is biased by a DC current I into a frequency f_J according to the Josephson equation

$$f_J = \frac{2e}{h} V_J \tag{3}$$

with e the elementary charge. For a voltage drop of 2 nV, a frequency of 1 MHz is generated. The voltage $V_J = IR$ is superimposed by the noise voltage of the resistor and hence, the frequency f_J is modulated by the noise. The noise voltage, which is a measure of the temperature T according to Eq. (2), can be obtained from the frequency fluctuations. To measure the frequency fluctuation precisely, parametric amplification is used. The RSQUID is coupled to a tank circuit and excited at its resonance frequency which results in a radiofrequency (rf) signal with sidebands reflecting the Josephson oscillation. After

demodulating the signal, a single sideband is filtered out using a band-pass filter. Now, amplitude fluctuations of the signal are no longer relevant and the frequency of the sideband is measured by a large number of frequency counts in a measuring time t_{meas} with a constant gate time τ of the counter. As a result, the temperature T can be determined from the variance of the repeated frequency counts with a relative statistical uncertainty given by the following equation

$$\frac{\Delta T}{T} = \sqrt{\frac{2\tau}{t_{\mathrm{meas}}}} \tag{3a}$$

Alternatively, because τ is related to the bandwidth Δf of the noise measurement, by

$$\frac{\Delta T}{T} = \frac{1}{\sqrt{t_{\mathrm{meas}}\Delta f}}. \tag{3b}$$

According to this formula, a temperature measurement with a statistical uncertainty of 10^{-3} and a practical gate time τ of 3 ms require a measuring time of about 15 h! These inconveniently long measurement times and additional problems with parasitic, non-thermal noise sources which have to be examined very carefully have restricted the use of these noise RSQUID thermometers to a very few metrology laboratories. Nevertheless, noise thermometry utilizing this type of a sophisticated mechanical SQUID played an important role in extending the ITS-90 to lower temperatures and establishing the PLTS-2000 [12, 1]. It should be noted that a modified version of a bulk rf RSQUID has been used for calorimetry at low temperature [13].

The concept of the RSQUID noise thermometer had been considered for practical thermometry at low temperature again at the end of the 1990s. Meanwhile, a reliable thin-film technology for DC SQUIDs emerged, which enabled the fabrication of integrated RSQUIDs. Different types of designs from both rf and DC RSQUIDs (here, the noise resistor is separating a two-junction SQUID loop) have been investigated intensively [14]. From a technological point of view, it was the crucial problem to integrate a low-ohmic resistorin the order of a few 10 μΩ into the SQUID loop. All sandwich-type resistors consisting of a metallic thin-film embedded in between two superconducting layers suffered from superconducting shorts caused by the proximity effect. This problem could be solved using a meander-like patterned metallic stripe with the current flow perpendicular to its long side [15]. Using this kind of noise resistors, integrated DC RSQUIDs have been developed that significantly simplified noise thermometer operation. It was shown theoretically that the main equations for noise thermometry deduced for rf RSQUIDs can also be applied to DC RSQUIDs. Experimentally, a relative uncertainty of the measured temperature of 6.6×10^{-3} could be achieved in 24 min and 10^{-3} was obtained in 15.5 h in a temperature range 140 mK to 5.9 K. Below 140 mK, hot electron effects and poor thermal coupling limit the precise operation of the devices [16].

Although the manufacture, experimental setup, and operation of the new generation of RSQUIDs were much more simple and reliable compared to bulky devices, the required measurement times were still quite long and the use in the typical temperature range of dilution refrigerators was hampered by inherent thermal problems. Because of these reasons, integrated RSQUIDs have neither gained significant recognition from potential users nor reached marketability. Attempts at fabricating RSQUIDs on the basis of high-T_c superconducting $YBa_2Cu_3O_{7-x}$ thin-films to address the temperature range above 4 K have been abandoned for technological reasons [17].

IV. CURRENT SENSING NOISE THERMOMETER

A. Principle

The current sensing noise thermometer (CSNT), where an LTS SQUID current sensor is used to measure the weak thermally activated noise current in resistor, has been introduced by Giffard *et al.* in the early 1970s. They have operated a bulk noise thermometer in a dilution refrigerator down to a temperature of 12 mK with the noise resistor in the mixing chamber [18, 19]. The principle of a CSNT is shown in Figure 3.

Fig. 3. Schematic diagram of a current sensing noise thermometer with a dc SQUID. R denotes the resistance of the noise resistor, L the inductance of the superconducting input coil, and M the mutual inductance between the input coil and the SQUID loop. The dotted lines enclose the parts of the setup which are at the same temperature stage **[20]**.

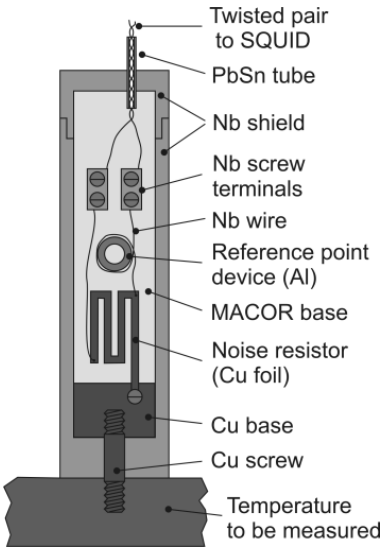

Fig. 4. CSNT version with a noise resistor made of 25 μm-thick copper foil grounded to a copper plate, obtained from **[20]**.

The thermal voltage noise in the resistor gives rise to fluctuating noise currents in the input coil of the SQUID current sensor with a total inductance L in the input circuit. The corresponding magnetic flux noise detected by the SQUID with mutual inductance M to the input coil is characterized by a first-order low-pass power spectral density (PSD)

$$S_\phi(f,T) = \frac{4k_\mathrm{B}TM^2}{R\left(1+\left(f/f_\mathrm{c}\right)^2\right)} \tag{4}$$

with a characteristic fall-off frequency $f_\mathrm{c} = R/(2\pi L)$ [20].

B. Practical versions of the CSNT

In practice, two types of CSNTs have been investigated, CSNTs with bulk noise resistors [20], [21], [22] and integrated thin-film devices [21]. At Royal Holloway University of London, CSNTs of the first type have been carefully designed and operated successfully over a wide temperature range from 4.2 K down to below 1 mK [20]. Relatively large noise resistors of a few milliohms could be used enabling short measuring times. The absolute temperature could be obtained in 10 s with a statistical uncertainty of about 1%. Figure 4 gives a diagram of this CSNT version. A main advantage of this thermometer is the non-dissipative operation of the noise resistor which makes it possible to use this thermometer at ultralow temperature. Nevertheless, in this temperature range, another problem arises from the weak electron-phonon coupling. In order to avoid electron overheating, the noise resistor is grounded at the copper plate which is held at the temperature to be measured. In order to provide an internal calibration point for this CSNT, a superconducting fixed point has been

implemented in the input circuit. Later implementations of the CSNT and its performance are described in [21] where a series with different noise resistors was investigated.

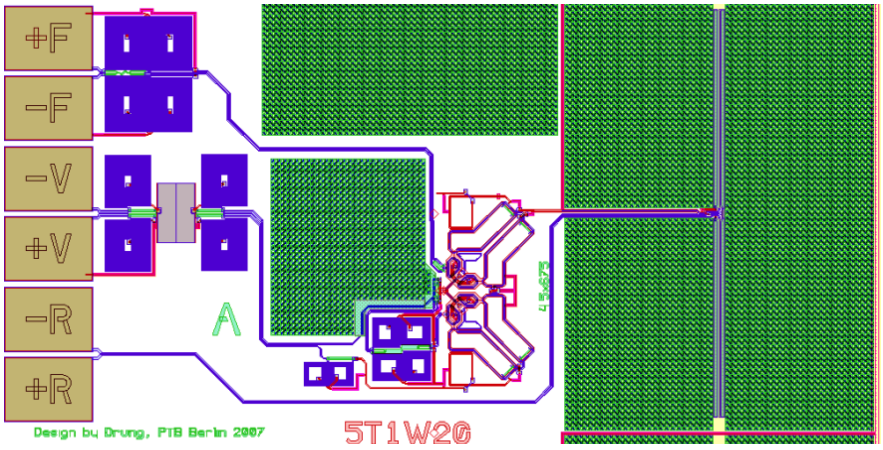

Fig. 5. Chip layout of an integrated thin-film dc SQUID CSNT [21]. The shaded areas represent the Pd noise resistor and bond pads for heat sinking whereas the dark blue objects on the left are filters. The bonding pads are located on the left chip side. The SQUID circuitry with the Josephson junctions is located in the lower middle of the chip.

Recently, integrated thin-film CSNTs have been manufactured at PTB on chips with a size of 2 mm × 3 mm which can be directly glued to the object whose temperature is to be measured, for example, a mixing chamber of a dilution refrigerator [23]. Because of the well-balanced gradiometric design of the integrated SQUID current sensor, no additional magnetic shielding is required. The noise resistor with a resistance of about 1 mΩ has been made of a Pd thin-film. In order to minimize hot electron effects, a large volume of 10^{-3} mm^3 has been spent for it. The large resistance results in very fast measuring times. Noise spectra are usually taken in an interval from 0 Hz to about 50 kHz. A statistical uncertainty of 1% can be achieved already in 33 ms. The measured temperature of the device has been found to be in good agreement with a high-accuracy realization of the PLTS-2000 in a temperature range down to 100 mK (well below 1% deviation). For even lower temperatures, a thermal decoupling of electrons in the noise resistor becomes measurable and deviations and uncertainties of the device increase. Improvements are expected by application of higher purity or another conductor material and larger volumes of the noise resistor. A separation of the thin-film noise resistor and the SQUID current sensor in a two-chip configuration with superconducting bonding wire connections is another option to avoid parasitic heating effects of the noise resistor. The chip layout is presented in Figure 5.

C. Primary mode CSNT

Recently, a CSNT version was investigated, which was operated in absolute primary mode [22]. This pCSNT was developed as a user-friendly thermometer, which can be easily optimized for a given temperature range by changing the noise resistor but also allows the

determination of all necessary system parameters to make it a primary device. The setup is similar to the one described in the previous subsection, but improved in many details. Figure 6 shows the schematic diagram of the pCSNT including data acquisition and processing to obtain the power spectrum density (PSD) $S_V(f)$ at the output of the FLL SQUID electronics. The PSD of the thermal noise currents flowing in the SQUID input circuit depends on both, the resistance R and the total inductance $L \geq L_{\mathrm{in}}$ in the input circuit:

$$S_I(f) = \frac{4k_{\mathrm{B}}T}{R}\frac{1}{1+(f/f_{\mathrm{c}})^2} \quad \text{with} \quad f_{\mathrm{c}} = \frac{R}{2\pi L}. \tag{5}$$

The relation between FLL output voltage, V, and the current in the input circuit, I_{in}, is given by the transresistance $A_{\mathrm{TR}} = V / I_{\mathrm{in}}$:

$$A_{\mathrm{TR}} = \frac{M_{\mathrm{in}}R_{\mathrm{f}}}{M_{\mathrm{f}}}, \tag{6}$$

where M_{in} is the mutual inductance between SQUID and input coil (L_{in}), M_{f} is the mutual inductance between SQUID and feedback coil, and R_{f} is the feedback resistor.
Combining Eq. (5) with Eq. (6), solving for T and introducing two corrections leads to the governing equation of the primary CSNT:

$$T_i = \frac{R}{4k_{\mathrm{B}}}\left(\frac{M_{\mathrm{f}}}{M_{\mathrm{in}}R_{\mathrm{f}}}\right)^2\left(1+\left(\frac{f_i}{f_{\mathrm{c}}}\right)^2\right)\left(S_V(f_i) - \left(\frac{R_{\mathrm{f}}}{M_{\mathrm{f}}}\right)^2 S_{\Phi,\mathrm{SQ}}(f_i)\right) - T_{\mathrm{g}}, \tag{7}$$

where f_i is the evaluated frequency, $S_{\Phi,\mathrm{SQ}}$ describes the additional flux noise introduced by the SQUID and SQUID electronics, and T_{g} is an effective temperature gradient between the platform temperature and the average temperature of the noise resistor. For absolute primary operation, all parameters occurring in Eq. (7) must be known or be determined under appropriate conditions. One effect neglected in Eq. (7) is an additional low pass behavior due to the bandwidth limitation of the FLL, $f_{\mathrm{c,FLL}}$, which depends on the SQUID characteristics at the working point, the feedback resistor R_{f} and the gain-bandwidth product of the SQUID electronics. For $f_{\mathrm{c,FLL}} \gg f_{\mathrm{c}}$, the deviation becomes reasonably small.

If other frequency-dependent effects, such as the skin effect in the resistor R, can be neglected, the low-pass behavior of the SQUID input circuit described by f_{c} is completely balanced by the corresponding behavior of S_V, resulting in temperature values T_i independent of the frequency f_i evaluated. In that case, f_{c} can be determined directly from S_V without the need to determine the total inductance L in the input circuit, which might be complicated.

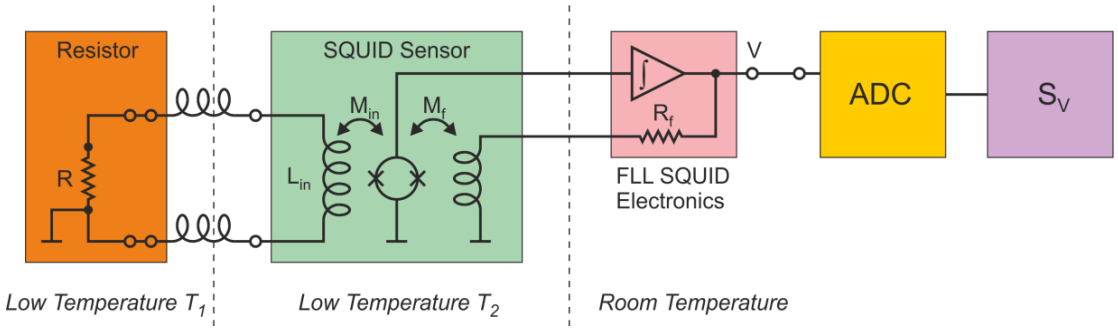

Fig. 6. Schematic of the CSNT. The noise current through the resistor R at temperature T_1 is measured by a SQUID current sensor at temperature T_2. The SQUID sensor is read out by a room-temperature SQUID electronics operated in FLL mode. The PSD SV to be evaluated is derived from the digitized output voltage V. All parts of the SQUID input circuit, except the resistor R and its link to ground, are superconducting.

In the pCSNT presented in [22], the resistor was made from a copper foil (99.99+% purity, 7.8 µm thickness), which was cut into a U-shape with one large area for heat sinking on one side. The resulting resistance was about 2 mΩ. Short superconducting NbTi wires (with CuNi clad) connected the resistor to a pair of screw terminals made of 70 µm Nb foil on a Stycast 1266 base, which provided reusable superconducting connections. The wire was soft soldered to the resistor and clamped in the terminal with the CuNi cladding removed using PEEK screws and square Nb washers. Further connection to the SQUID used a twisted pair of NbTi wire without cladding, which was threaded through a thin niobium tube, filled with Apiezon N grease. The sensor base, which is mounted to the platform (temperature T_1 in Figure 6) and hosts the resistor, was made of annealed OFHC copper. A Nb tube serves as a magnetic shield. A two-stage, double-transformer SQUID current sensor of PTB type "XL" [24] with an input inductance of L_{in} = 1.05 µH was used for the readout. The SQUID sensor was mounted in a magnetic shield at the cold plate (continuous heat-exchanger plate) of a dilution refrigerator, where the temperature (T_2 in Figure 6) varies between 100 mK and 300 mK. In this temperature range, the SQUID noise can be considered essentially constant as the SQUID (junction shunts) does not cool effectively below 300 mK. At that temperature, the SQUID noise is typically 0.26 $\mu\Phi_0/\mathrm{Hz}^{1/2}$ at 100 kHz and increases towards lower frequencies. A constant noise level of $S_{\Phi,\mathrm{SQ}}$ = 1.0 $\mu\Phi_0/\mathrm{Hz}^{1/2}$ was assumed for the SQUID noise contribution.

According to Eq. (7), besides R, the two SQUID-related parameters M_{in} and M_f had to be determined. The resistance measurement on R was made with the assembled CSNT resistor thermalized at the temperature-stabilized mixing chamber plate using the 4-wire technique and lock-in readout of the voltage drop across R. The resistance was measured between 20 mK and 1 K with a relative uncertainty of 0.68%. The mutual inductance M_{in} was measured by applying a slowly changing current ΔI_{in} to the SQUID input coil and counting the corresponding number n of flux quanta Φ_0. This was done with the SQUID electronics being operated in the reset mode and thus resolving the flux-to-voltage characteristics of the

SQUID. The mutual inductance is then given by $M_{in} = n\Phi_0 / \Delta I_{in}$. By counting about 440 flux quanta, the resulting relative uncertainty was 0.30%. Within the measurement uncertainty, no temperature dependence was observed between 7.5 mK and 1 K. For the measurement of M_f it is important to consider the residual coupling between input coil and feedback coil despite a SQUID design reducing this interaction as much as possible. This means that M_f depends on the load connected to the input coil, resulting in a difference of about 0.6% of M_f between open and shorted input coil. Hence, the measurement of M_f was performed *in situ*, with the pCSNT assembled and the resistor connected as shown in Figure 6. The SQUID electronics XXF-1 [25] was used in FLL mode with activated autoreset function to provide a current to the feedback coil and measure the voltage difference needed to apply an integral number of flux quanta. This method resulted in a relative uncertainty of 0.58% for M_f. There was no observable temperature dependence between 20 mK and 0.7 K. The value of the feedback resistor is associated with an uncertainty of 0.06% [26].

The pCSNT investigated in [22] used a resistor of about 2 mΩ, which results in a bandwidth of $f_c \approx 230$ Hz. It was estimated for an earlier CSNT design with $R = 1.95$ mΩ, based on a comparison with a platinum NMR thermometer below 1 mK, that at 20 mK, a CSNT of that design exhibits a temperature gradient of 6.6 μK across the resistor, if a constant heat leak is assumed. Primary temperature measurements were reported between 0.21 K and 35 mK in comparison with PLTS-2000 temperatures provided by a superconducting reference device. Spectra with at least 14×200 averages consisting of up to 2^{19} points were obtained within the range 48 mHz … 25 kHz, and non-thermal interference peaks were filtered out.

According to the uncertainty budget given for 20 mK, the largest uncertainty components (in terms of relative contribution to the combined uncertainty) result from M_f (61%), R (21%), M_{in} (16%) and S_V (1.8%). All other components contribute with less than 1%. At 20 mK the relative combined standard uncertainty is 1.53% (coverage factor $k = 1$). A comparison of the pCSNT with the PLTS-2000 between 0.21 K and 66 mK confirmed a good agreement within the combined standard uncertainties, although the pCSNT temperature values were systematically higher by approximately 0.8%.

V. MAGNETIC FIELD FLUCTUATION THERMOMETER

A. Principle

The Brownian motion of charge carriers in a conductor at a given temperature causes magnetic field fluctuations above the surface of the conductor. These magnetic field fluctuations are sometimes called *magnetic* Johnson–Nyquist noise. Its noise power and (temporal) frequency spectrum in a point at a distance z above the surface is determined by the geometry and electrical conductivity σ of the conductor, the distance z, and temperature.

The basic working principle of a MFFT is to detect the magnetic Johnson–Nyquist noise in the vicinity of a conductor inductively and to extract the conductor temperature. The conductor is the actual temperature sensor, and it is in tight thermal contact with the object, the temperature of which is to be measured.

B. Practical versions of the MFFT

MFFTs for the low (<4.2 K) temperature range have been developed. Their two essential components are a temperature sensor made of a material with an electrical conductivity highly constant in the temperature range of interest, and a magnetometer sensitive enough to detect the magnetic Johnson–Nyquist noise. Noble metals are widely used materials in cryotechnics. They can be prepared in high purity and typically show both a high and a close-to-constant conductivity at low temperatures. A SQUID-based magnetometer is the natural sensor for the low-temperature MFFT, as it combines very high sensitivity and operability in the relevant temperature range. The first low-temperature MFFT configuration [27] consisted of a temperature sensor in the form of a metallic cylinder made of high-purity gold surrounded by a pickup coil of niobium wire. This coil was connected to the input of a SQUID current sensor. The pickup coil and the SQUID input formed a superconducting flux transformer that coupled the magnetic Johnson–Nyquist noise into the SQUID loop. In a more compact implementation, a chip with an integrated SQUID magnetometer is placed directly onto the temperature sensor. This configuration has a number of advantages. A lithographically fabricated pickup coil can be designed more precisely and more flexibly with respect to the geometry of the temperature sensor. Also, the SQUID sensor is operated at the temperature to be measured. This makes it possible that the SQUID noise reduces with temperature over a significant range toward lower MFFT operation temperature.

An easy-to-use noise thermometer system, MFFT-1, has been developed specifically for use in modern sub-kelvin refrigerators and commercialized [28]. Its main component is the sensor module comprising a copper temperature sensor, a SQUID sensor chip, and a superconducting magnetic shield. The system also includes EMI-shielded cryostat cabling, SQUID-readout electronics, and data acquisition and analysis software. The high-purity copper temperature sensor has a volume of 1.2 cm^3. The SQUID sensor chip (size 3.3 mm × 3.3 mm) is affixed directly onto the Cu body. The magnetic Johnson–Nyquist noise integrated over the effective, magnetic-field-sensitive area of the SQUID is detected as a magnetic flux noise. The SQUID sensor is specifically designed to be used in an MFFT. It is a concentric multiloop radial gradiometer and represents a trade-off between a desirably strong inductive coupling to the thermal noise currents in the temperature sensor and a reduced sensitivity to background magnetic fields inside the refrigerator. The module is easily mounted, for instance to the mixing chamber plate of a dilution refrigerator, with the threaded stud at the end of the Cu body. The Cu body underneath the location of the SQUID sensor has a reduced thickness of about 0.2 mm. In conjunction with the Cu conductivity and the distance of the SQUID sensor to the Cu body (≈100 μm), this leads to a magnetic Johnson–

Nyquist noise at 1 K with a root mean square (rms) flux value of typically about 15 mΦ_0 in the SQUID, the precise value depending on the exact SQUID-to-Cu body distance of a given MFFT-1 module (Figure 7).

In order to extract the temperature information from the magnetic Johnson–Nyquist noise, the noise frequency spectrum is analyzed, although a time-domain analysis would be equally applicable. The noise spectra are obtained from time series of the SQUID sensor signals that are transformed into the frequency domain by fast Fourier transformation. The individual spectra of N_{Avg} time series are then rms-averaged with equal weighting. The MFFT noise spectra show a "low-pass-like" frequency dependence. They can be analyzed in a model-based "parametric" manner as well as in a "nonparametric" way (see below). In the parametric approach, the frequency dependence of the noise PSD is parameterized using the expression

$$S_{\Phi}\left(T,f\right)=\frac{s_0 T}{\left(1+\left(2f/\pi f_{\mathrm{c}}\right)^{2p_1}\right)^{p_2}} \tag{8}$$

Here, s_0T denotes the zero-frequency value of the flux noise PSD, and the parameters f_{c}, p_1, and p_2 are used to describe the frequency dependence. For a fixed sensor module geometry, the parameters f_{c}, p_1, and p_2 are independent of temperature, provided that σ does not vary with T. This means that, for $\sigma = \mathrm{const}(T)$, the PSD at any frequency is directly proportional to T.

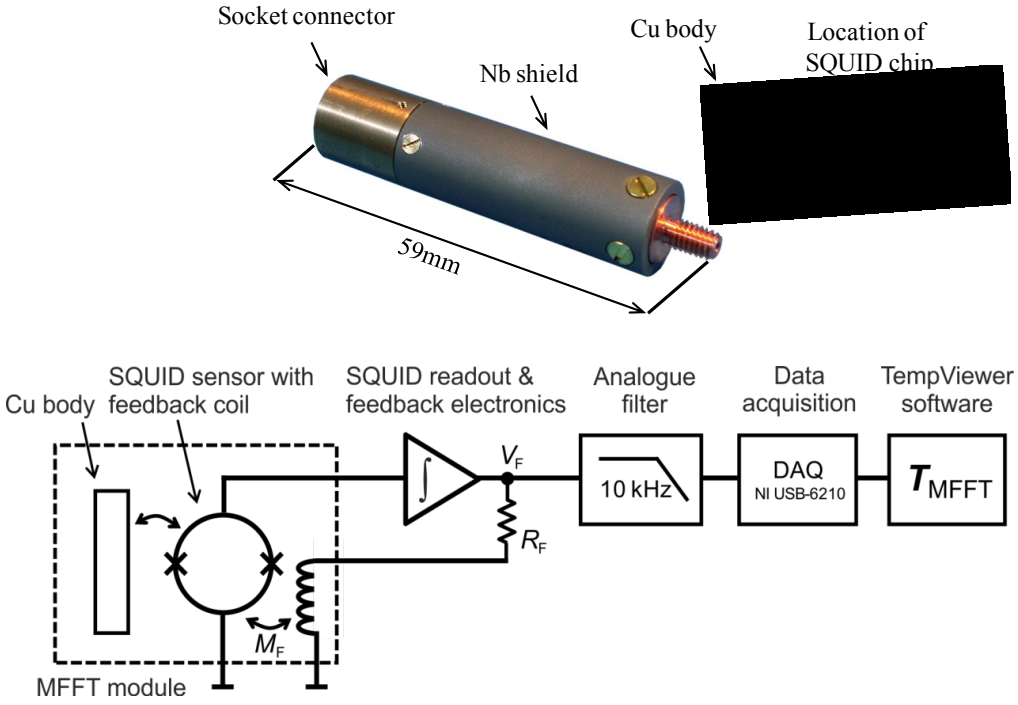

Fig. 7. Sensor module, Cu temperature sensor, and measurement block diagram of the MFFT-1 thermometer developed for the temperature range of about 1 K to 10 mK [26].

Furthermore, only one reference measurement at a known temperature T_{ref} is needed to obtain the set of calibration parameters s_0, f_c, p_1, and p_2 that characterize a given MFFT-1 sensor module. The estimate T_{MFFT} of an unknown temperature T is obtained by way of comparing the noise spectrum measured at T with the reference spectrum measured at T_{ref}. The simple thermometer function

$$T_{\mathrm{MFFT}} = \frac{S_0(T)}{S_0(T_{\mathrm{ref}})} T_{\mathrm{ref}} = \frac{S_0(T)}{s_0} \tag{9}$$

is obtained, when the zero-frequency value of the flux noise power spectrum is used as the basis of this comparison, although the same relation holds for the thermal noise at any frequency. In practice, the zero-frequency bin of the flux noise power spectrum may be "contaminated" by non-thermal noise. Then, the calibration parameter s_0 – together with f_c, p_1, and p_2 – can be obtained by means of fitting the model expression of Eq. (8) to the reference noise spectrum $S(T_{\mathrm{ref}},f)$ within a frequency range Δf that may not include the zero-frequency bin.

In a nonparametric analysis, it still is preconditioned that the sensor module geometry and the Cu conductivity σ do not change in the operational temperature range. However, it is not attempted to model the PSD frequency dependence. The PSD values measured at temperature T of N_{f} bins within Δf are individually compared to the corresponding PSD values of the reference measurement spectrum. Then, N_{f} temperature estimates are obtained that can be analyzed – in the simplest approach by averaging – to determine the estimate $\hat{T}$ of the unknown temperature.

It is clear from the thermometer function of Eq. (9) that MFFT-1 temperature measurements with high accuracy require a correspondingly precise knowledge and realization of at least one reference temperature T_{ref}. The (relative) uncertainty of the reference temperature $u_{\mathrm{rel}}(T_{\mathrm{ref}})$ sets the lower limit to the uncertainty of the temperature estimate T_{MFFT} obtained. Consideration of the statistics of the data acquisition and analysis of the spectra with both the model-based and the nonparametric analysis shows that the relative uncertainty $u_{\mathrm{rel}}(T_{\mathrm{MFFT}})$ can be expressed as

$$u_{\mathrm{rel}}^2(T_{\mathrm{MFFT}}) = \left(\frac{u(T_{\mathrm{MFFT}})}{T_{\mathrm{MFFT}}}\right)^2 \approx \frac{1}{N_{\mathrm{f}} N_{\mathrm{Avg,meas}}} + \frac{1}{N_{\mathrm{f}} N_{\mathrm{Avg,ref}}} + u_{\mathrm{rel}}^2(T_{\mathrm{ref}}) \tag{10}$$

where N_{f} denotes the number of frequency bins of the reference and measurement spectra that are evaluated, and $N_{\mathrm{Avg,meas}}$ and $N_{\mathrm{Avg,ref}}$ are the numbers of time traces measured to obtain the spectra. The first and second uncertainty contributions in Eq. (10) represent the statistics of a measurement at the temperature to be determined and of the reference measurement, respectively. When $N_{\mathrm{Avg,meas}} \ll N_{\mathrm{Avg,ref}}$, and furthermore $1/\sqrt{(N_{\mathrm{f}}\ N_{\mathrm{Avg,ref}})} \approx u_{\mathrm{rel}}(T_{\mathrm{ref}})$, the

uncertainty of the MFFT measurement is dominated by the statistics – that is, the measurement time – with which the noise spectrum $S(T,f)$ is acquired. Uncertainty contributions that arise from the noise of the SQUID sensor (and its room temperature readout electronics) are neglected in expression (10). Doing so is justified because the MFFT-1 noise temperature is sufficiently low. The noise temperature is the temperature $T_{\mathrm{Noise,MFFT}}$ at which the magnetic Johnson–Nyquist noise would equal the SQUID sensor noise. As can be seen in Figure 8, the MFFT-1 noise temperature $T_{\mathrm{Noise,MFFT}}$ is below 100 μK for the frequency range $\Delta f \approx 10$ Hz to 3.5 kHz. The low end of the intended range of MFFT-1 operation is a few millikelvin. Therefore, the SQUID sensor noise contribution can be safely disregarded. In practical temperature measurements with the MFFT-1 relative uncertainties of <1% can be obtained within a few seconds to a few tenths of a second, assuming a resolution bandwidth of 1 Hz.

As discussed above, a meaningful determination of the MFFT-1 temperature estimate T_{MFFT} preconditions that the temperature sensor conductivity $\sigma = \mathrm{const}(T)$ and that the temperature sensor and SQUID magnetometer configuration does not change after the reference measurement. The same conditions must be fulfilled for the mutual inductance between SQUID and feedback coil, M_{F}, and for the feedback resistor, R_{F}, see Figure 7. Violation of these conditions would compromise the linearity of thermometer function. The T_{MFFT} has been found to be highly linear in comparison with the temperature of a high-accuracy realization of the PLTS-2000 at PTB [29].

Moreover, the traceability of the MFFT to the PLTS-2000 has been demonstrated [26]. The reference temperature was realized by highly precise superconducting reference points. This is a well-established method to disseminate the PLTS-2000 with low uncertainty [30]. Calibration against the PLTS-2000 yields relative uncertainties of the reference temperatures of superconducting reference points of typically 2×10^{-4} [30] which hence limits the achievable uncertainty in this calibration procedure.

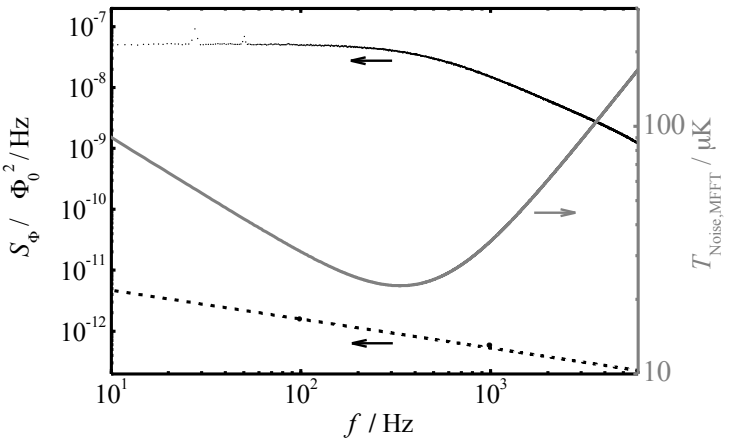

Fig. 8. Magnetic flux noise spectrum S_Φ measured for a MFFT-1 sensor module at the superconducting transition temperature of a Zn reference sample $T = 848.64$ mK (black dots). The black dashed line shows a representative flux noise spectrum of the SQUID sensor of MFFT-1 sensor modules. The

gray curve is the SQUID noise temperature $T_{Noise,MFFT}$ calculated from the SQUID sensor flux noise and the temperature independent frequency response of the magnetic Johnson noise [26].

C. Primary mode MFFT

The MFFTs introduced in the preceding subsection are based on a thermometer function like Eq. (9), which relates the ratio of flux noise density $S_\Phi(T)$ and temperature T to the corresponding ratio $S_\Phi(T_{ref}) / T_{ref}$ obtained at a known reference temperature T_{ref}. This operation as *relative primary thermometer* assumes that all relevant parameters with influence on the gain of the signal chain (see Figure 7) can be considered as constant. In this case, the value of the frequency dependent ratio $g(f) = S_\Phi(f, T) / T$ is not depending on the temperature T. This requires that the electrical conductivity σ and the magnetic permeability μ of the temperature sensor as well as the coupling of the thermal noise flux into the detection coil are independent of T. Furthermore, if the MFFT's SQUID sensor can change its temperature, the mutual inductances between SQUID and feedback coil, M_f, and (for SQUID current sensors) between SQUID and input coil, M_{in}, must also be independent of T.

In order to operate a MFFT as an *absolute primary thermometer,* the ratio $g(f)$ above must be known with reference to the Boltzmann constant k_B, independent of any temperature fixed point. For such a primary MFFT (pMFFT) this means that $g(f)$ is determined based on the geometry and the electrical conductivity of the temperature sensor, the geometry of the detection coil and the calibration of the SQUID gradiometer with readout electronics, which detects the thermal noise flux. Since the determination of $g(f)$ can be very challenging for arbitrary geometries, an appropriate design of the pMFFT can help to simplify the comprehensive and exact determination of the geometries and to reduce the complexity of the necessary (mathematical) calculations. For this reason, the optimization of a pMFFT may have slightly different goals as for the MFFT.

Another aspect of designing the pMFFT is the reduction of the thermometer noise temperature. As discussed in the preceding subsection, the noise temperature $T_{Noise,MFFT}$ is determined by the SQUID sensor noise. This parameter quantifies a Type B uncertainty component for T_{MFFT}. It is comprehensible that $T_{Noise,MFFT}$ should be adequately low with regard to the designated accuracy of the pMFFT at the minimum temperature of operation. A method to minimize the noise temperature (theoretically to zero) is based on cross-correlation. In 1959 Fink proposed and demonstrated this technique to eliminate the contributions of lead resistance and amplifier noise in Johnson noise thermometry down to 1.3 K [31]. The cross-correlation technique was used in [32] in a MFFT setup for sub-millikelvin thermometry and enabled one to measure temperatures as low as 50 μK.

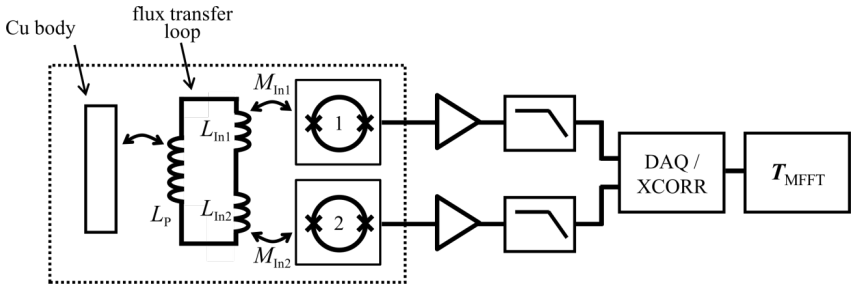

Fig. 9. Measurement block diagram of the correlation-based MFFT readout. The detection coil with inductance L_P and the input coils of two identical SQUID sensors 1 and 2 with $M_{In1} = M_{In2}$ form a superconducting flux transfer loop. The two channels are read out independently. A two-channel data

acquisition system (DAQ) is used to digitize the output signals and analyze their cross-correlation (XCORR) to extract the temperature of the Cu temperature sensor.

One possible cross-correlation scheme for the MFFT is depicted in Figure 9. The magnetic Johnson–Nyquist noise of the temperature sensor produces magnetic flux in the detection coil with inductance L_P. This coil together with the superconducting input coils of two identical SQUID current sensors with $M_{In1} = M_{In2}$ form a superconducting flux transfer loop. This way the thermal noise signals of which the temperature is extracted are entirely correlated in the two SQUID sensors. Both channels are read out independently, and a two-channel data acquisition system is used to digitize the SQUID output signals. Hence, the readout noise contributions (intrinsic noise of the SQUID sensors, readout electronic and DAQ) occur, in principle, completely uncorrelated in the output signals. Note, that the two SQUID sensors are inductively coupled which each other via the flux transfer loop. This will, depending on the dimensioning of the flux transfer loop, lead to some degree of correlation of the nominally uncorrelated readout noise contributions. Notwithstanding this, analyzing the cross-correlation of the SQUID signals to extract the temperature suppresses the effect of the 'non-thermal' readout noise drastically.

A pMFFT for the temperature range of the PLTS-2000 has been developed for metrological application [33, 34]. This pMFFT uses the cross-correlation technique with two independent channels and is based on two planar thin-film detection coils, read out by SQUID current sensors. Sensor and coil geometries have been chosen to enable feasible analytical electromagnetic modeling, but not primarily to achieve very low single-channel noise temperatures. In addition, it has a separate calibration coil, which is used to determine the electrical conductivity of the temperature sensor and the flux-to-voltage (i.e., calibration) coefficients of the two SQUID gradiometer channels.

The temperature is evaluated from the cross-correlated signal $S_{V,12}$, which is closely related to the cross-power spectral density (CPSD) $S_{\Phi,12}$ of the thermal magnetic flux noise (TMFN) in the detection coils. The real part of the cross-correlated signal $\mathrm{Re}[S_{V,12}(f)]$ ($\sim \mathrm{Re}[S_{\Phi,12}(f)]$) enters in equation (11) to calculate the temperature value, while $\sigma(T)$, and the channel calibration depend only weakly on temperature and are determined separately. The SQUID current sensors are operated in a closed-loop feedback mode with feedback into the superconducting input circuit (input current-lock, ICL). This readout scheme is essential for the pMFFT due to two reasons: Within the ICL bandwidth (i) the flux transfer from the detection coil into the SQUID is independent of frequency and (ii) the interaction between both detection coils and between detection coils and metallic temperature sensor is suppressed. This has the consequence that (i) the detection coils can be modeled as virtually open circuit with no current flowing and (ii) the weak or vanishing interaction between both signal channels makes them effectively independent, which is a necessary condition for the cross-correlation technique. A special design of the detection coils, which cancels the magnetic interaction between both channels at dc and low frequencies, supports the

decoupling of the signal channels. Each SQUID input circuit is equipped with an additional RC shunt to limit the bandwidth of the input circuit.

The temperature is calculated according to

$$T = \frac{\hat{V}_{\mathrm{Rcal},1} \cdot \hat{V}_{\mathrm{Rcal},2} \cdot M_1 \cdot M_2}{\hat{V}_{\mathrm{cal},1} \cdot \hat{V}_{\mathrm{cal},2} \cdot R_{\mathrm{cal}}^2} \cdot T_{\mathrm{Ref}} \cdot \frac{1}{N_f} \sum_{k=1}^{N_f} \frac{\mathrm{Re}\left[S_{V,12}(f_k, V_1, V_2)\right]}{\mathrm{Re}\left[S_{\Phi,12}(f_k, \sigma, T_{\mathrm{Ref}}, \ldots)\right]} \tag{11}$$

where N_f denotes the number of frequency bins considered for evaluation, $S_{V,12}$ is the CPSD of the measured voltages, and $S_{*,12}$ is the calculated CPSD of the TMFN in the detection coils at an arbitrary temperature T_{Ref}. R_{cal} is the value of the resistor used to measure the current through the calibration coil, M_1 and M_2 are calculated values (based on the geometry) of the mutual induction between calibration coil and the respective detection coil. The other quantities are determined during calibration using quasi-dc currents: $V_{\mathrm{cal},i}$ is the voltage of the signal channel i, while $V_{\mathrm{Rcal},i}$ is the corresponding voltage drop at the calibration resistor. Although a reference temperature T_{Ref} occurs in Eq. (11), it cancels out because $\mathrm{Re}[S_{*,12}(f, \sigma, T_{\mathrm{Ref}}, \ldots)] \propto T_{\mathrm{Ref}}$.

The TMFN $S_{*,12}$ is calculated based on the geometry and the electrical conductivity of the temperature sensor and the geometry of the detection coil. Since the realized geometries are rather simple, the temperature sensor can be approximated as (infinite) slab, and the detection coils can be modeled as filamentary conductors with contours c_1 and c_2. Under these assumptions, the TMFN can be solved analytically and evaluated numerically without the need to perform elaborate finite-element method (FEM) calculations. The solution is of the form

$$S_{\Phi,12}(f) = S_{\Phi}(f, c_1, c_2) = {\mu_0}^2 \sigma k_{\mathrm{B}} T \cdot F(c_1, c_2, \mu_0 \sigma f, \ldots), \tag{12}$$

,

where $F(\ldots)$ is a complex-valued function depending on the whole geometry and the product $\mu_0 \sigma f$. Flux focusing in the superconducting multi-turn coils is considered separately as correction.

An alternative way to calculate the TMFN, favorable but not only useful for FEM calculations, is based on [35]:

$$S_{\Phi} = \frac{4 k_{\mathrm{B}} T \,\mathrm{Re}(Z)}{(2\pi f)^2} = \frac{4 k_{\mathrm{B}} T}{(2\pi f)^2} \cdot \frac{\mathrm{Re}(P)}{I^2} \tag{13}$$

On the right side of Eq. (13) the real part of the complex impedance, $\mathrm{Re}(Z)$, is replaced by the dissipation power inside the temperature sensor divided by the square of the exciting ac

current I flowing through the detection coil. The complex power P is obtained from the solution of the corresponding eddy current problem in the temperature sensor.

The pMFFT sensor shown in Figure 10 is machined from a copper cylinder with a diameter of 18 mm and a length of 100 mm. High-purity copper with nominal 99.9998% purity and a residual resistivity ratio of about 100 is used. The cylinder has large openings from opposite sides to take up the two coil chips (39 mm × 13 mm) and printed circuit boards (PCBs) that host the SQUID sensors. The body of the pMFFT has two cut-outs, where the SQUID sensors and bond loops are located in a central position. The remaining material in between (and below the detection coils) forms the actual temperature sensor. This part has a thickness of about 2 mm and a lateral size of 11 mm (13 mm) × 18 mm. The two Si chips that host the detection coils and the calibration coil are mounted face down from opposite sides parallel to the surface of the temperature sensor. They are pressed by springs made of $CuSn_6$ onto a 1 mm-wide raised rim, which defines the gap between chips and temperature sensor. The gap size is ≈100 µm on one side and ≈50 µm on the opposite side, while the two coil chips can be applied on either side.

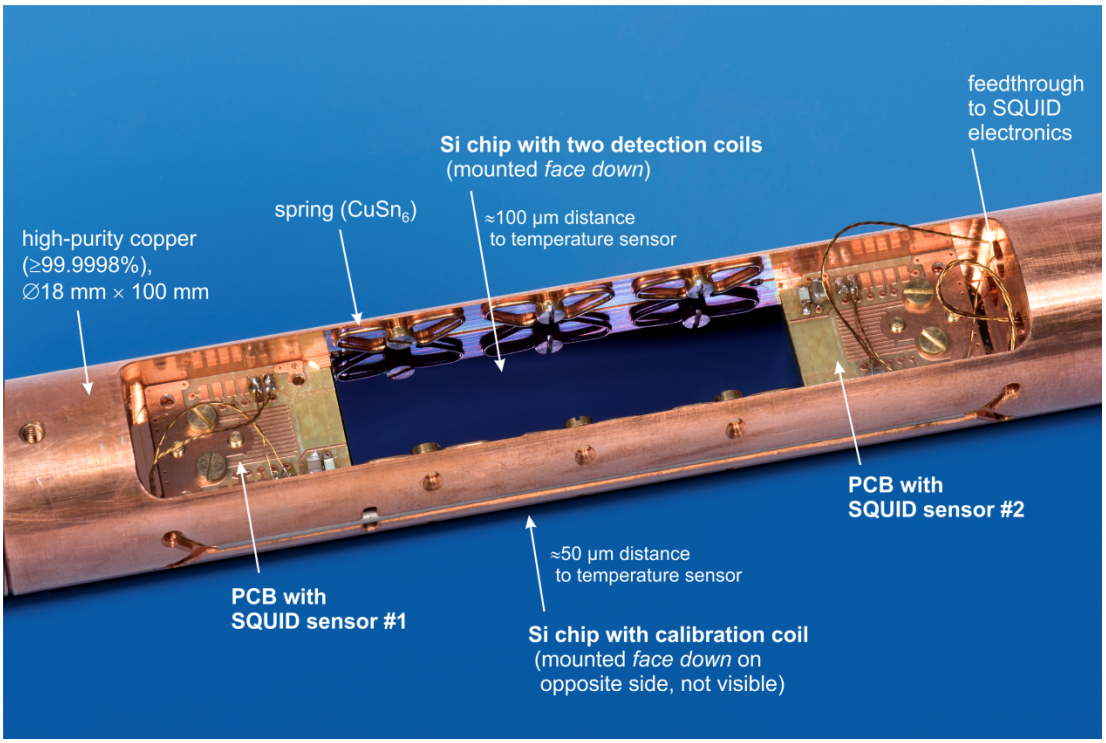

Fig. 10. Inside view of the pMFFT body without magnetic shielding. The two SQUID sensors and the bond connections to the Si chips are not visible because they are located on the back side of the PCBs.

The coils are fabricated on Si wafers with standard Nb thin-film technology, making use of the (sub-)micrometer precision of photolithography. The minimum linewidth used and gaps between the lines are 3 µm. All coils are realized as series gradiometers, which are described by a single current. The coaxial gradiometers minimize the magnetic coupling to

the far environment, and their circular shape is one condition to solve the eddy current problem analytically. The coplanar arrangement with interleaved turns of both detection coils permits a large magnetic coupling and thus a high correlation for the TMFN, while the capacitive coupling remains relatively low. The outer diameter of the gradiometer is about 4 mm. In order to minimize the overall magnetic coupling between both signal channels, each detection coil consists of two identical gradiometers in series with suitable polarity. One gradiometer pair is placed above the temperature sensor to detect the TMFN, whereas the other one is located above the cut-out and counterbalances the magnetic coupling of the first gradiometer. The estimated total coil inductance is about 400 nH. Readout is performed by single-stage, double-transformer SQUID current sensors from PTB of type "L" [24].

Primary temperature measurements with the pMFFT were reported in [34] between 0.7 K and 16 mK. CPSD spectra with up to 51100 averages were obtained within the range 0.61 Hz … 5000 Hz, and non-thermal interference peaks (e.g. at the mains frequency and harmonics) were filtered out. As the value of the electrical conductivity used in Eq. (12) was determined directly from the CPSD using a fit procedure and not taken from the integral conductivity measurement, the frequency range for the temperature calculation with Eq. (11) was confined to 420 Hz … 3600 Hz. These evaluation steps are illustrated in Figure 11, which shows the spectrum (CPSD) of the thermal noise and the corresponding temperature values for a measurement at ≈16 mK.

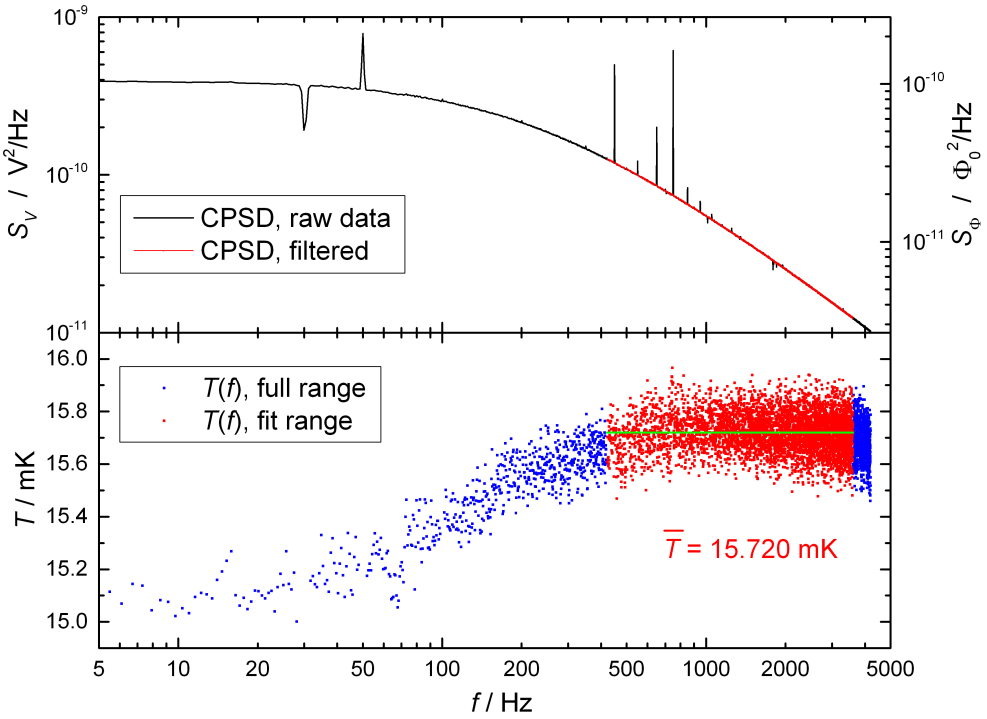

Fig. 11. Thermal noise and temperature spectra at about 16 mK. The upper diagram shows the CPSD after 51100 averages. The black curve is the raw data. After filtering out non-thermal interference peaks and confining the frequency range to 420 Hz … 3600 Hz, the red curve is obtained. The right scale corresponds to the SQUID-referred CPSD. The lower diagram shows the corresponding temperature values. The frequency bins in the confined range, marked by the red dots, are used for the

temperature calculation, which involves a fit procedure to obtain the correct conductivity value. This fit results in a "flat" temperature spectrum within the evaluated (confined) range, while a deviating spectrum can evolve outside.

According to the uncertainty budget given for 16 mK, the largest uncertainty components (in terms of relative contribution to the combined uncertainty) result from the distances between detection coils and calibration coil (84%) and between detection coils and sensor surface (9%), the ac voltage measurement (ADC gain, flatness) (3%), the electrical conductivity (2%), the radii of the calibration coil (1.4%) and the radii of the detection coils (0.14%). All other components such as various edge effects due to the model approximations in Eq. (9) are still much smaller. At 16 mK the relative combined standard uncertainty is 0.59% (coverage factor k = 1). Due to the linear characteristic of the pMFFT and the practically temperature-independent uncertainty contributions, this relative uncertainty holds for the entire operation range of the pMFFT. A comparison of the pMFFT with the PLTS-2000 between 672 mK and 16 mK confirmed a good agreement within the combined standard uncertainties. Nonetheless, at 16 mK a slight tendency to lower pMFFT temperatures was observed.

VI. CONCLUSIONS

As it was described at the beginning of this article, SQUID based thermometry played an important role already in establishing the low-temperature scale PLTS-2000. For this purpose, bulky RSQUIDs with a mechanically adjustable Josephson contact were applied. Those devices were developed and used already in the 70th and 80th of the last century. Later on, modern thin-film device technology enabled the manufacture of thin-film RSQUIDs, but it turned out that these devices cannot be used practically below 100 mK due to limitations caused by hot electron effects in the thin-film resistor.

At the beginning of this century, low-noise dc-SQUID-sensor-based thermometers were developed for Johnson noise thermometry down to about 10 mK. Theses practical noise thermometers, the CSNT and the MFFT are reliable, comparably easy-to-use and suitable for operation in all types of state-of-the art cryostats including those utilizing mechanical cryo-coolers.

In comparison with the CSNT, the MFFT configuration eliminates the need for galvanic contacts to the metallic temperature sensor. This is a practical advantage as it avoids potential effects of the contacts, such as nonohmic contact resistances, as well as contamination of the temperature sensor. Also, the sensor may have a larger volume compared to small thin-film resistors typically used in a CSNT and a RSQUID noise thermometer. This provides for better thermal anchoring of the temperature sensor, which is the more important the lower the temperature to be measured.

The CSNT and MFFT have been operated so far mostly as relative primary thermometers, which are calibrated against the PLTS-2000 at only one reference temperature.

For the majority of users this is acceptable and does not hamper their practical application. If required, these thermometers can be operated in an absolute primary mode. This has been demonstrated in the PLTS-2000 temperature range both for the CSNT and the MFFT, independently. The pCSNT discussed in 4.2 is based on the same technical setup as its relative primary version. Absolute primary mode requires the independent determination of the values of the noise resistor, the SQUID input and feedback coupling and the feedback resistor with low uncertainty. The pMFFT implementation described in 5.2 allows the *in situ* determination of the resistivity of the temperature sensor as well as of coupling coefficient. This enables the user to check the integrity of the thermometer in operation.

The pCSNT and the pMFFT allow the measurement of the thermodynamic temperature T in the range of the PLTS-2000 with relative uncertainties of about 1%. They are being used to investigate existing discrepancies in the PLTS-2000 background data. In addition, both thermometer types have the potential to support the extension of the temperature scale below 0.9 mK, the lower end of the PLTS-2000. Their operation in this ultra-low temperature range has already been demonstrated. It is foreseeable that by using the cross-correlation approach effective noise temperatures sufficiently low to measure temperatures of some tens of microkelvin with percent-range relative uncertainty is possible.

REFERENCES

[1] G. Schuster, D. Hechtfischer and B., Fellmuth, "Thermometry below 1 K". *Rep. Prog. Phys.*, **57**, 187–230 (1994).

[2] Y. Maeno, H. Haucke, H., and J. Wheatley, "Simple differential thermometer for low temperatures using a thermocouple with a SQUID detector". *Rev. Sci. Instrum.*, **54**, 946 (1983).

[3] H.R. Naren, R.S. Sannabhadti, A. Kumar,V. Arolkar, A. de Waard, G. Frossati, and S. Ramakrishan, "Setting up of a microKelvin refrigerator facility at TIFR". *Curr. Sci.*, **101**, 28–34 (2011).

[4] H. Preston-Thomas "The international temperature scale of 1990 ITS-90". Metrologia, 27, 3–10 and 107 (erratum) (1990).

[5] R L. Rusby, M. Durieux, A.L. Reesink, R. P. Hudson, G. Schuster, M. Kühne, W.E. Fogle, R. J. Soulen, and E.D. Adams, "The provisional low temperature scale from 0.9 mK to 1 K, PLTS-2000." *J. Low Temp. Phys.,* **126**, 633–642 (2002).

[6] R. L. Rusby, B. Fellmuth, J. Engert W. E. Fogle, E.D. Adams, L. Pietre, and M. Durieux, "Realization of the 3He melting pressure scale, PLTS-2000." *J. Low Temp. Phys.*, **149**, 6156–6175 (2007).

[7] J. Engert, B. Fellmuth, and K. Jousten, "A new 3He vapour-pressure based temperature scale from 0,65 K to 3.2 K consistent with the PLTS-2000". *Metrologia,* **44**, 40–52 (2007).

[8] B. Fellmuth, J. Fischer, C. Gaiser, O. Jusko, T. Priruenrom, W. Sabuga, and T. Zandt, "Determination of the Boltzmann constant by dielectric-constant gas thermometry". *Metrologia*, **48**, 382–390 (2011).

[9] B. Fellmuth, J. Fischer, G. Machin, S. Picard, P.P.M. Steur, O. Tamura, D.R. White, and H. Yoon, "The kelvin redefinition and its mise en pratique". *Phil. Trans. R. Soc. A.*, **374**, 20150037 (2016).

[10] R.A. Kamper and J.E. Zimmerman, "Noise thermometry with the Josephson effect". *J. Appl. Phys.*, **42**, 132–136 (1971).

[11] A. Hoffmann and B. Buchholz, "UHF-resistive noise thermometer at temperatures between 0.005 and 4.2 K". *J. Phys. E: Sci. Instrum.*, **17**, 1035–1037 (1984).

[12] R.J. Soulen, Jr., W.E. Fogle, and J.H. Colwell, "Measurements of absolute temperatures below 0.75 K using a Josephson noise thermometer". *J. Low Temp. Phys.*, **94**, 385–487 (1994).
[13] J.G. Park, and A.W. Vaidya, "Resistive SQUID calorimetry at low temperatures". *J. Low Temp. Phys.*, **40**, 247–274 (1980).
[14] G.S. Krivoy, C. Assmann, M. Peters, and H. Koch, "Design and fabrication of thin-film resistive SQUIDs". *J. Low Temp. Phys.*, **99**, 107 (1995).
[15] S. Menkel, D. Drung, C. Assmann, and T. Schurig, "A dc resistive SQUID noise thermometer". *Appl. Supercond.*, **6**, 417 (1998).
[16] S. Menkel, D. Drung, Y.S. Greenberg, and T. Schurig, "Integrated thin-film dc RSQUIDs for noise thermometry". *J. Low Temp. Phys.*, **120**, 381–400 (2000).
[17] D.A. Peden, J.C. Macfarlane, L. Hao, R.P. Reed, and J.C. Gallop, "YBCO – Noble metal resistors for HTS Josephson noise thermometry". *IEEE Trans. Appl. Supercond.*, **9**, 4408–4411(1999).
[18] R.P. Giffard, R.A. Webb and J.C. Wheatley, "Principles and methods of low-frequency electric and magnetic measurements using an rf-biased point contact superconducting device". *J. Low Temp. Phys.*, **6**, 533–610 (1972).
[19] R.A. Webb, R.P. Giffard, and J.C. Wheatley, "Noise thermometry at ultralow temperatures". *J. Low Temp. Phys.*, **13**, 383–429 (1973).
[20] C.P. Lusher, J. Li, V.A. Maidanov, M.E. Digby, H. Dyball, A. Casey, J. Nyeki, V.V. Dimitriev, B.P. Cowan, and J. Saunders, "Current sensing noise thermometry using a low T_c DC SQUID preamplifier". *Meas. Sci. Technol.*, **12**, 1–15 (2001).
[21] A. Casey, F. Arnold, L.V. Levitin, C.P. Lusher, J. Nyéki, J. Saunders, A. Shibahara, H. van der Vliet, B. Yager, D. Drung, T. Schurig, G. Batey, M.N. Cuthbert, and A.J. Matthews, "Current Sensing Noise Thermometry: A Fast Practical Solution to Low Temperature Measurement". *J. Low Temp. Phys.*, **175**, 764-775 (2014).
[22] A. Shibahara, O. Hahtela, J. Engert, H. van der Vliet, L.V. Levitin, A. Casey, C.P. Lusher, J. Saunders, D. Drung and T. Schurig, "Primary current-sensing noise thermometry in the millikelvin regime". *Phil. Trans. R. Soc. A.,* **374**, 20150054 (2016).
[23] J. Engert, J.,Beyer, D. Drung, A. Kirste, D. Heyer, A. Fleischmann, C. Enss and H.-J. Barthelmess, "Practical noise thermometers for low temperatures". *J. Phys. Conf. Ser.*, **150**, 012012 (2009).
[24] D. Drung, C. Aßmann, J. Beyer, A. Kirste, M. Peters, F. Ruede, and T. Schurig, "Highly sensitive and easy-to-use SQUID sensors". *IEEE Trans. Appl. Supercond.*, **17(2),** 699-704 (2007).
[25] Magnicon Magnicon XXF-1, http://www.magnicon.com/squid-electronics/xxf-1/
[26] J. Beyer, M. Schmidt, J. Engert, S. AliValiollahi, and H.-J. Barthelmess, "Reference measurements of SQUID-based magnetic-field fluctuation thermometers". *Supercond. Sci. Technol.*, **26**, 065010 (2013).
[27] A. Netsch, E. Hassinger, C. Enss and A. Fleischmann, "Novel, non-contact noise thermometer for Milli-kelvin temperatures". *AIP Conf. Proc.,* **850**, 1593 (2006).
[28] Magnicon Magnicon MFFT-1, http://www.magnicon.com/squid-systems/noise-thermometer/
[29] J. Engert, J., Beyer, D. Drung, A. Kirste, and M. Peters, "A noise thermometer for practical thermometry at low temperatures". *Int. J. Thermophys.*, **28**, 1800 (2007).
[30] J. Engert, D. Heyer, and J. Fischer, "Low-temperature thermometry below 1 K at PTB". *AIP Conf. Proc.* **1552**, 136 (2013).
[31] H. J. Fink "A New Absolute Noise Thermometer at Low Temperatures". *Canadian Journal of Physics*, **37**, 1397-1406 (1959).
[32] D. Rothfuß, A. Reiser, A. Fleischmann, and C. Enss, "Noise thermometry at ultra low temperatures". *Appl. Phys. Lett* **103**, 052605 (2013).
[33] A. Kirste, M. Regin, J. Engert, D. Drung, and T. Schurig, "A calculable and correlation-based magnetic field fluctuation thermometer". *J. Phys.: Conf. Ser.*, **568**, 032012 (2014).
[34] A. Kirste, and J. Engert, "A SQUID-based primary noise thermometer for low-temperature metrology". *Phil. Trans. R. Soc. A.,* **374**, 20150050 (2016).

[35] J.T. Harding, J.E. Zimmerman, "Quantum interference magnetometry and thermal noise from a conducting environment". *Phys. Lett.* **27A**, 670-671 (1968).